Preparation and characterization of mesoporous Lanthanum-doped bioactive glass nanoparticles

A. Z. Ashemary[a,b,*] S. M. Haidary[c], Y. Muhammed[d], İ. S. Çardakli[e]
[a]*Department of Chemistry, College of Science, Mathematics and Technology, Wenzhou-Kean University, Wenzhou 325060, China*
[b]*Biomedical Engineering Department, College of Engineering and Technologies, Al-Mustaqbal University, Hillah 51001, Babil, Iraq*
[c]*Department of Food Technology, College of Agricultural Engineering Sciences, Salahaddin University, Erbil, Iraq*
[d]*Aeronautical Techniques Engineering, AL-Farahidi University, Baghdad, Iraq.*
[e]*Department of Metallurgical and Materials Engineering, Atatürk University,Erzurum, 25240, Turkey*

In this study, novel compositions of mesoporous Bioglass (BG) and Lanthanum-doped BG (La-BG) were prepared using the sol-gel method. Microstructure analysis of the produced composites was performed using XRD, FESEM, FTIR, TGA, and BET techniques. The XRD patterns of BG and La-BG show a good match with the combeite phase. The silicate and phosphate groups in the BG and La-BG lattice were detected in FTIR spectra. The BG particles were spherical, with a surface area of 11.54 m^2/g, a pore volume of 0.02491cc/g, and a pore size of 31.35Å. With the addition of La, the BG structure revealed (i) increased crystallinity of diffraction peaks, (ii) the particles changed from a spherical to a petal-like shape with an expansion in surface area and pore volume, and (iii) increased thermal stability of the BG structure. In conclusion, BG's physiochemical characteristics were greatly enhanced by adding La.

(Received February 13, 2023; Accepted May 18, 2023)

Keywords: Bioglass, Lanthanum, Sol-gel, Characterizations

1. Introduction

Bioactive glass (BG) is a bioactive ceramic material that binds to host hard tissues. It's a quaternary system synthesized by Hench with an appropriate composition of SiO_2, CaO, Na_2O, and P_2O_5 with outstanding bioactivity and osteoconductivity [1, 2]. Numerous studies have shown that a scaffold made of BG can support bone and dental implants. Cordioli et al. demonstrated that mineralized tissue of adequate quality and volume is produced when BG and autogenous bone are mixed in a 4:1 ratio, as is usually done to improve the maxillary sinus floor [3]. In a 12-month clinical and radiographic investigation, Mengel et al. presented the findings on using a bioabsorbable membrane and BG in treating intrabody damage in people with severe periodontitis. Results from a 5-year follow-up revealed considerable increases in clinical indicators in each of these investigations, demonstrating the ability of BG in the regenerative repair of periodontal lesions [4].

Two different methods were used to synthesize BG particles. In the melt-quenching method, constituent oxides are melted in a platinum crucible, drastically reducing the powder's porosity, and thus not a viable option for many applications [5]. While the sol-gel method requires lower temperatures than melt quench synthesis, a mixture of metal–organic and metal salts are used as a precursor. Heat treatment is necessary once a gel has been formed by hydrolysis and condensation processes [6]. The latter method is preferred because it allows greater control over the product's composition and homogeneity. The obtained BG materials from the sol-gel method have a porous structure with a more comprehensive range of bioactivity, a higher surface area, and

* Corresponding author: aalshema@kean.edu
https://doi.org/10.15251/DJNB.2023.182.681

significantly improved surface activity. Breaking down this BG releases calcium, silica, salt, and phosphate, which combine with ions to generate carbonated hydroxyapatite (C-HA), causing a larger degree of interaction with the natural tissue and the ensuing increased binding to biological tissues. This process culminates in the C-HA layer forming strong connections with the nearby bone, which promotes and stimulates bone formation [7].

However, using BG materials is frequently linked to poor mechanical and antibacterial properties. Based on these drawbacks, various authors suggested modification of the structure of BG via doping metallic and non-metallic oxides into the composition of the BG lattice. This doping can provide the glass with other capabilities, including angiogenesis and antibacterial properties. Due to their impact on osteogenesis and angiogenesis, several metallic ions, including copper, gallium, strontium, silver, cobalt, cerium, magnesium, and zinc, have been incorporated into BG, demonstrating that the addition of these ions improves physical characteristics and therapeutic properties [8-14].

Lanthanum ions (La^{3+}), its rare earth element, have recently attracted increasing attention for tissue engineering applications. It's been linked to strong mechanical and bactericidal properties, fast wound healing, anti-inflammatory properties, healing impact, bioactivity, and biocompatibility when utilized in repairing skin tissues and functioning the system of life [15]. Furthermore, it was found that the addition of La^{3+} ions improved the thermal stability, flexural strength, and biocompatibility of the apatite structure [16]. Joshy et al. proved that adding La^{3+} ions to the HA lattice sustained the release of the amoxicillin drug [17]. It was demonstrated that adding La onto Ti substrates with HA coatings improved cell proliferation and osteogenic differentiation [18]. La^{3+} ions have shown a possible inclination to increase the proliferation and induce the osteogenic differentiation of human adipose-derived mesenchymal cells before using a powerful osteoinductive medication like dexamethasone. It has also been proven that rat osteoblasts and mouse primary bone marrow stromal cells respond to La^{3+} ions by undergoing osteogenic differentiation [19]. It has also been shown that lanthanum oxide may enhance the glass transition temperature and thermal stability of iron phosphate glasses [20].

Thus, the primary purpose of this work was to create and describe La modified with doping as a component for synthesis and to assess the effect of dopants on the physiochemical characteristics of the BG structure.

2. Materials and method

2.1. Materials

TEOS ($SiC_8H_{20}O_4$), TEP ($C_6H_{15}O_4P$), $Ca(NO_3)_2.4H_2O$ and $NaNO_3$, and $La(NO_3)_3.6H_2O$ were used as source of SiO_2, P_2O_5, CaO, NaO, and La_2O_3, respectively. 1M of HNO_3 was used to hydrolyze the TEOS.

2.2. Synthesis Bioglass and Lanthanum Doped Bioglass

The sol-gel method was used to make BG and La-doped BG. 1 M HNO_3 (2.25 mL) in H_2O (48.6 mL) was mixed with 33.5 mL of TEOS. Hydrolysis of the precursor permitted 60 minutes of reaction. The following reagents were stirred separately for 45 minutes: 2.9 ml TEP, 20.13 g $Ca(NO_3)_2$, and 13.52 g $NaNO_3$. The clear sol was enclosed in a container for 5 days at ambient temperature to make the gel. The gel was aged in a sealed container at 70°C for one day and then dried at 120°C for one day in a drying oven. To eliminate residual nitrates, the dried sample was stabilized at 800°C in a benchtop muffle furnace for 2 h, as summarized in Figure 1. La-doped BG was prepared using the same steps, and the amounts of $Ca(NO_3)_2$ and $La(NO_3)_3$ were 10.03 g and 17.32 g, respectively.

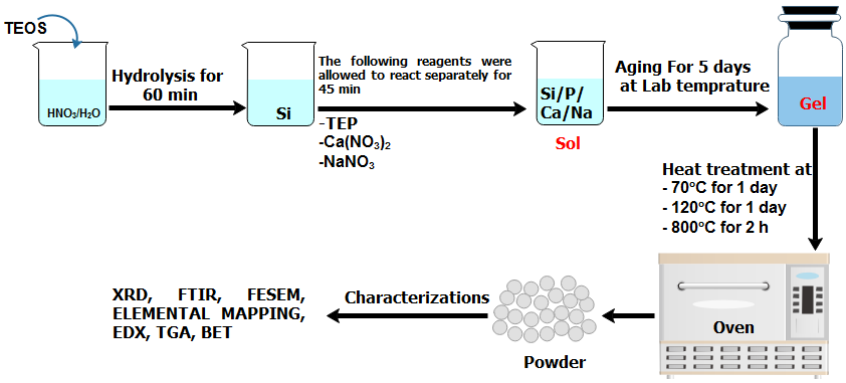

Fig. 1. Experiment flow chart.

2.3. Characterizations

The BG and La-BG samples were characterized using a different analytical approach. The materials' phase purity was evaluated with an X-ray diffractometer (XRD), scanned at intervals of 0.03° from 20° to 80°. Utilizing Fourier transform infrared spectroscopy (FTIR) allowed for identifying the frequencies of the powder's functional group vibrations. It was necessary to use a field emission scanning electron microscope ((FESEM) to study the structure and elemental mapping of the prepared materials. The powders were sonicated in 20 mL of 100% ethanol for 30 minutes to break up clumps and then dried at room temperature for FESEM analysis. Thermogravimetric analysis (TGA) was used to investigate the thermal stability of the produced materials. The temperature range for this investigation was from room temperature to 950°C, and sample weights were recorded throughout the investigation. Using Brunauer, Emmett, and Teller's formulas (BET-Multiple point), powder's pore volume, size, and surface area were measured.

3. Results and discussion

The XRD patterns of the BG and La-BG produced using the sol-gel method are shown in Figure 2. Crystallization is typical for BG subjected to heat at temperatures over 800 °C [21]. The patterns match the standard of the crystalline phase $Na_2Ca_2Si_3O_9$ (combeite) (JCDPS No. 075-1687), resulting in a matrix containing an amorphous phase rich in phosphorous. The prominent sharp peaks were located at 33.6° and 34.2°, attributed to the diffraction planes of (024) and (220), respectively. Combeite is formed in the greatest quantity possible at about 800°C because to CaO depletion, glass has become less stable [22]. Furthermore, along with the combeite phase, a crystalline apatite-like phosphorous-rich phase ($Na_2Ca_4(PO_4)_2SiO_4$ (JCDPS No. 032 1053)) was also detected. The increased intensity of these peaks after La was injected into the BG lattice provided conclusive evidence that La had been effectively incorporated into the BG structure.

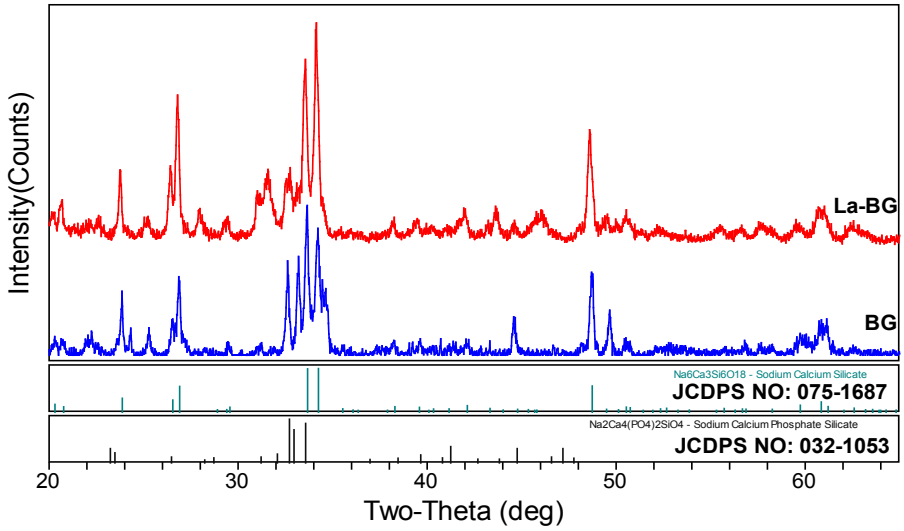

Fig. 2. XRD patterns of BG and La-BG materials.

The BG particles were found to be aggregated spheres with a mean diameter of 237 nm (Fig. 3). The morphology and particle size changed significantly with the incorporation of La. The BG particles partially changed from spherical to petal-like particles with adding La. The elemental mapping analysis confirmed the homogeneity of elemental distribution in the representative sample (Fig. 3).

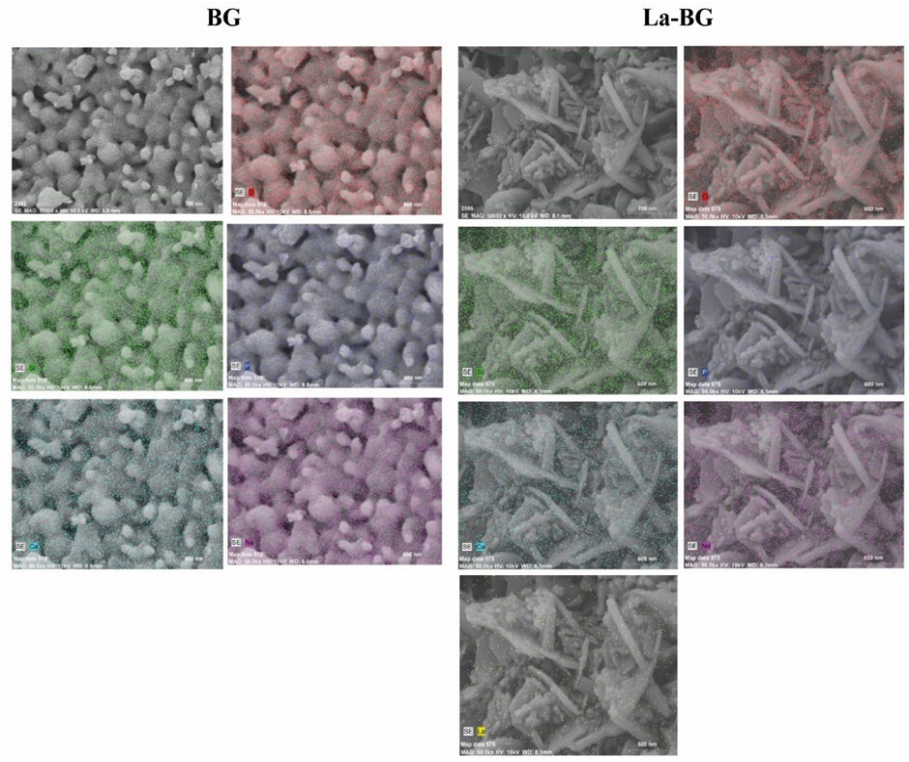

Fig. 3. FESEM images and elemental mapping of BG and La-BG materials.

Figure 4 displays the FTIR spectra of BG and La-BG. Since Si-O is stretched asymmetrically, acoustically dominant bands between 766 and 1175 cm^{-1} may be seen. Another prominent peak, at 1443 cm^{-1}, may represent the Si-O-Si vibration band. The two peaks at 611 and

692 cm^{-1} caused by P-O bending in phosphate. The 611-692 cm^{-1} absorption band was linked to the PO_4^{3-} antisymmetric bending, demonstrating that phosphorus is present as orthophosphate. The hygroscopic character of silicate glasses is shown by detecting water's O-H symmetric stretching vibration modes in the range of 3613 cm^{-1} in these materials [21].

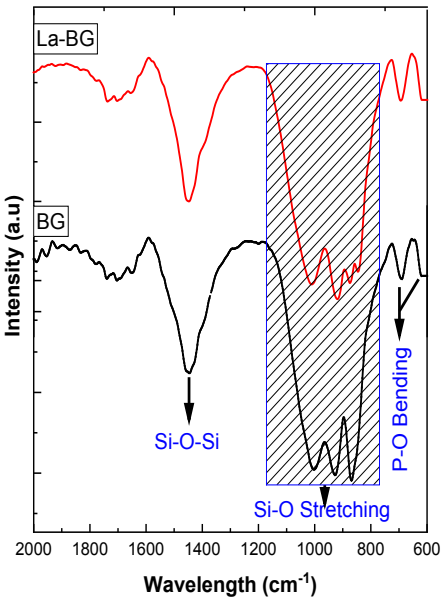

Fig. 4. FTIR spectra of BG and La-BG materials.

To learn more about how well something resists heat, TGA was employed to investigate BG and La-BG materials (Figure 5). The TGA curves of the crystals can be separated into three distinct temperature ranges as follows: (A) 30°C–151°C, which links to the loss of adsorbed water from the surface of samples [23]; (B) 151°C–264°C, which indicates the loss of lattice water and organic species; and (C) 264°C–714°C, which illustrates the loss of nitrate molecules. It was revealed that a larger proportion of weight was lost across the board when La was added to BG structure.

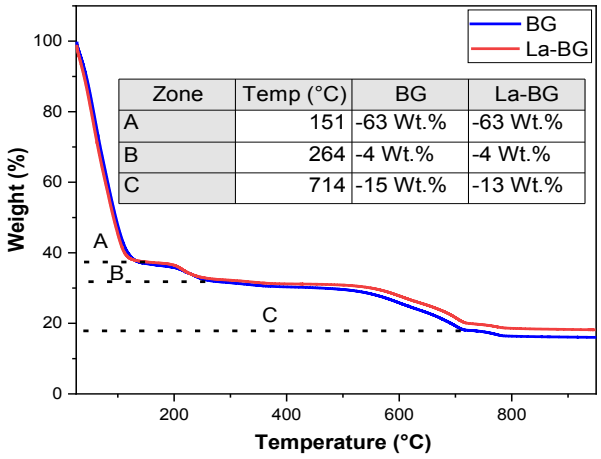

Fig. 5. TGA graph of BG and La-BG materials.

To get a textural profile of the materials, nitrogen adsorption and desorption isotherms were used. Figure 6 illustrates the adsorption and desorption isotherms for nitrogen that may be

obtained from the materials. Because the BG and La-BG isotherms are both of the type IV sorts, the materials at issue are considered to be mesoporous according to the classification method used by IUPAC. One-dimensional channels may be readily recognized by their characteristic curves, which are type H1 hysteresis loops. This allows for quick and simple identification. As can be seen in Table 1, the surface area, the pore volume, and the average pore diameter were all calculated by the process of nitrogen adsorption. When the concentration of La was increased, the surface area boosted from 11.54 m^2/g to 16.69 m^2/g. Pore volume statistics confirm this idea. This led to a rose in the pore volume, which went from 0.02491 cc/g to 0.03563 cc/g as a direct effect. As a result of the incorporation of La, the mesoporous silica saw an increase in its specific surface area and pore volume, which is evidence of structural disruption. The average pore diameter also grew from 31.35 to 39.25Å [21].

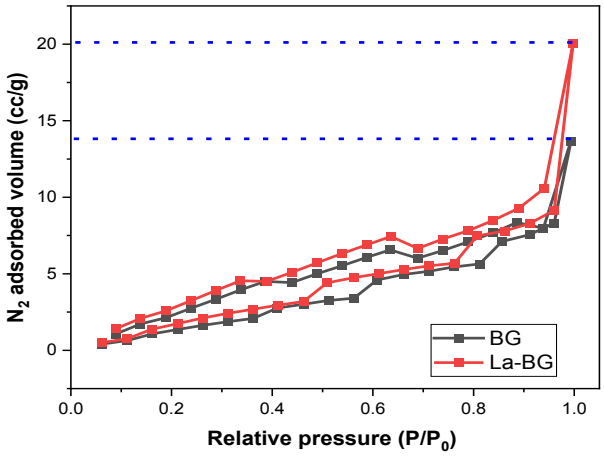

Fig. 6. N_2 adsorption–desorption isotherm.

Table 1. Textural parameters obtained by N_2 adsorption measurement.

	BG	La-BG
Surface Area Data		
Multipoint BET	11.54 m²/g	16.69 m²/g
BJH Method Cumulative Adsorption Surface Area	14.15 m²/g	17.56 m²/g
BJH Method Cumulative Desorption Surface Area	23.11 m²/g	24.79 m²/g
DH Method Cumulative Adsorption Surface Area	14.52 m²/g	18.11 m²/g
DH Method Cumulative Desorption Surface Area	25.38 m²/g	27.35 m²/g
DR Method Micro Pore Area	10.21 m²/g	13.33 m²/g
Pore Volume Data		
BJH Method Cumulative Adsorption Pore Volume	0.02491 cc/g	0.03563 cc/g
BJH Method Cumulative Desorption Pore Volume	0.02868 cc/g	0.03830 cc/g
DH Method Cumulative Adsorption Pore Volume	0.02424 cc/g	0.03460 cc/g
DH Method Cumulative Desorption Pore Volume	0.02906 cc/g	0.03847 cc/g
DR Method Micro Pore Volume	0.003637 cc/g	0.004747cc/g
Pore Size Data		
BJH Method Adsorption Pore Diameter (Mode)	31.35 Å	39.25 Å
BJH Method Desorption Pore Diameter (Mode)	21.33 Å	23.93 Å
DH Method Adsorption Pore Diameter (Mode)	31.35 Å	39.25 Å
DH Method Desorption Pore Diameter (Mode)	21.33 Å	23.93 Å
DR Method Micro Pore Width	76.77 Å	78.20 Å
DA Method Pore Diameter (Mode)	30.20 Å	30.60 Å
HK Method Pore Width (Mode)	18.52 Å	17.58 Å
SF Method Pore Diameter (Mode)	34.37 Å	33.45

4. Conclusion

This research used a sol-gel technique to create mesoporous bioactive glass particles containing lanthanum. Glass's textural features, such as its specific surface area, were improved due to lanthanum's inclusion in the amorphous structure. The findings obtained demonstrated that La affected the microstructure of BG. In light of these encouraging findings, researchers plan to examine the bioactivity of these materials to determine if they can be used as multifunctional implants capable of fostering bone growth and eliciting a local hyperthermic effect, both crucial to overcoming bone cancer and curing the disease.

Acknowledgements

Dr. Ammar Z. Alshemary would like to thank Al-Mustaqbal University.

References

[1] L.L. Hench, Journal of the american ceramic society, 74 1487-1510 (1991); https://doi.org/10.1111/j.1151-2916.1991.tb07132.x

[2] V. Krishnan, T. Lakshmi, Journal of advanced pharmaceutical technology & research, 4, 78 (2013); https://doi.org/10.4103/2231-4040.111523

[3] G. Cordioli, C. Mazzocco, E. Schepers, E. Brugnolo, Z. Majzoub, Clinical oral implants research, 12, 270-278 (2001); https://doi.org/10.1034/j.1600-0501.2001.012003270.x

[4] R. Mengel, D. Schreiber, L. Flores-de-Jacoby, Journal of periodontology, 77, 1781-1787 (2006); https://doi.org/10.1902/jop.2006.060029

[5] G. Kaur, G. Pickrell, N. Sriranganathan, V. Kumar, D. Homa, Journal of Biomedical Materials Research Part B: Applied Biomaterials, 104, 1248-1275 (2016); https://doi.org/10.1002/jbm.b.33443

[6] K. Deshmukh, T. Kovářík, T. Křenek, D. Docheva, T. Stich, J. Pola, RSC advances, 10, 33782-33835 (2020); https://doi.org/10.1039/D0RA04287K

[7] M. Cannio, D. Bellucci, J.A. Roether, D.N. Boccaccini, V. Cannillo, Materials, 14, 5440 (2021); https://doi.org/10.3390/ma14185440

[8] Y.F. Goh, A.Z. Alshemary, M. Akram, M.R. Abdul Kadir, R. Hussain, International Journal of Applied Glass Science, 5, 255-266 (2014); https://doi.org/10.1111/ijag.12061

[9] Y.-F. Goh, A.Z. Alshemary, M. Akram, M.R. Abdul Kadir, R. Hussain, Materials Chemistry and Physics, 137, 1031-1038 (2013); https://doi.org/10.1016/j.matchemphys.2012.11.022

[10] Y.-F. Goh, A.Z. Alshemary, M. Akram, M.R. Abdul Kadir, R. Hussain, Ceramics International, 40, 729-737 (2014); https://doi.org/10.1016/j.ceramint.2013.06.062

[11] T. Keenan, L. Placek, A. Coughlan, G. Bowers, M. Hall, A. Wren, Carbohydrate polymers, 153, 482-491 (2016); https://doi.org/10.1016/j.carbpol.2016.07.100

[12] S.A. Mosaddad, M. Yazdanian, H. Tebyanian, E. Tahmasebi, A. Yazdanian, A. Seifalian, M. Tavakolizadeh, Journal of Materials Research and Technology, 9, 14799-14817(2020); https://doi.org/10.1016/j.jmrt.2020.10.065

[13] J.R. de Souza, E.C. Kukulka, J.C.R. Araújo, T.M.B. Campos, R.F. do Prado, L.M.R. de Vasconcellos, G.P. Thin, A.L.S. Borges, Journal of Biomedical Materials Research Part B: Applied Biomaterials, 111, 151-160 (2023); https://doi.org/10.1002/jbm.b.35141

[14] Z. Huan, S. Leeflang, J. Zhou, W. Zhai, J. Chang, J. Duszczyk, Journal of Biomedical Materials Research Part B: Applied Biomaterials, 100, 437-446 (2012); https://doi.org/10.1002/jbm.b.31968

[15] Y. Liu, Q. Zhang, N. Zhou, J. Tan, J. Ashley, W. Wang, F. Wu, J. Shen, M.J.C.E.J. Zhang, 395, 125059 (2020); https://doi.org/10.1016/j.cej.2020.125059

[16] D. Guo, A. Wang, Y. Han, K.J.A.B. Xu, 5, 3512-3523 (2009);

https://doi.org/10.1016/j.actbio.2009.05.026
[17] M.A. Joshy, K. Elayaraja, R. Suganthi, S.C. Veerla, S.N.J.C.A.P. Kalkura, 11, 1100-1106 (2011); https://doi.org/10.1016/j.cap.2011.02.003
[18] W. Lou, Y. Dong, H. Zhang, Y. Jin, X. Hu, J. Ma, J. Liu, G. Wu, International journal of molecular sciences, 16, 21070-21086 (2015); https://doi.org/10.3390/ijms160921070
[19] X. Wang, L. Yuan, J. Huang, T.L. Zhang, K.J.J.o.c.b. Wang, 105, 1307-1315 (2008); https://doi.org/10.1002/jcb.21932
[20] B. Qian, X. Liang, S. Yang, S. He, L.J.J.o.M.S. Gao, 1027, 31-35 (2012); https://doi.org/10.1016/j.molstruc.2012.05.078
[21] Y.-F. Goh, A.Z. Alshemary, M. Akram, M.R.A. Kadir, R. Hussain, Ceramics International, 40, 729-737 (2014); https://doi.org/10.1016/j.ceramint.2013.06.062
[22] H. Pirayesh, J.A. Nychka, Journal of the American Ceramic Society, 96, 1643-1650 (2013); https://doi.org/10.1111/jace.12190
[23] Y.M. A. Z. Alshemary, İ. S. Çardakli, A. B. Marandi, Digest Journal of Nanomaterials and Biostructures, 18, 1-10 (2023); https://doi.org/10.15251/DJNB.2023.181.1